Acinetobacter baumannii Catabolizes Ethanolamine in the Absence of a Metabolosome and Converts Cobinamide into Adenosylated Cobamides

Elizabeth A. Villa,[a] Jorge C. Escalante-Semerena[a]

aDepartment of Microbiology, University of Georgia, Athens, Georgia, USA

ABSTRACT *Acinetobacter baumannii* is an opportunistic pathogen typically associated with hospital-acquired infections. Our understanding of the metabolism and physiology of *A. baumannii* is limited. Here, we report that *A. baumannii* uses ethanolamine (EA) as the sole source of nitrogen and can use this aminoalcohol as a source of carbon and energy if the expression of the *eutBC* genes encoding ethanolamine ammonia-lyase (EAL) is increased. A strain with an IS*Aba1* element upstream of the *eutBC* genes efficiently used EA as a carbon and energy source. The *A. baumannii* EAL (*Ab*EAL) enzyme supported the growth of a strain of *Salmonella* lacking the entire *eut* operon. Remarkably, the growth of the above-mentioned *Salmonella* strain did not require the metabolosome, the reactivase EutA enzyme, the EutE acetaldehyde dehydrogenase, or the addition of glutathione to the medium. Transmission electron micrographs showed that when *Acinetobacter baumannii* or *Salmonella enterica* subsp. *enterica* serovar Typhimurium strain LT2 synthesized *Ab*EAL, the protein localized to the cell membrane. We also report that the *A. baumannii* genome encodes all of the enzymes needed for the assembly of the nucleotide loop of cobamides and that it uses these enzymes to synthesize different cobamides from the precursor cobinamide and several nucleobases. In the absence of exogenous nucleobases, the most abundant cobamide produced by *A. baumannii* was cobalamin.

IMPORTANCE *Acinetobacter baumannii* is a Gram-negative bacterium commonly found in soil and water. *A. baumannii* is an opportunistic human pathogen, considered by the CDC to be a serious threat to human health due to the multidrug resistance commonly associated with this bacterium. Knowledge of the metabolic capabilities of *A. baumannii* is limited. The importance of the work reported here lies in the identification of ethanolamine catabolism occurring in the absence of a metabolosome structure. In other bacteria, this structure protects the cell against damage by acetaldehyde generated by the deamination of ethanolamine. In addition, the ethanolamine ammonia-lyase (EAL) enzyme of this bacterium is unique in that it does not require a reactivase enzyme to remain active. Importantly, we also demonstrate that the *A. baumannii* genome encodes the functions needed to assemble adenosylcobamide, the coenzyme of EAL, from the precursor cobinamide.

KEYWORDS *Acinetobacter baumannii*, ethanolamine catabolism, ethanolamine ammonia-lyase, cobinamide salvaging, metabolosome, bacterial microcompartments, nucleotide loop assembly, B$_{12}$ biosynthesis, cobamide, ethanolamine ammonia-lyase reactivation, metabolosomes

A cinetobacter baumannii is a nonmotile Gram-negative bacillus of concern to public health due to its ability to rapidly develop resistance to antibiotics, leading to multidrug-resistant strains that are difficult to treat. At present, *A. baumannii* is listed

FIG 1 Comparison of the *eut* genes in *S.* Typhimurium and *A. baumannii*. (A) In *S.* Typhimurium, a total of 17 gene functions are needed for ethanolamine utilization (*eut* genes) as a carbon, nitrogen, and energy source under certain growth conditions. (B) In contrast, *A. baumannii* may require seven or fewer putative *eut* genes to break down ethanolamine. Genes are at the scale indicated by the bar.

as a high-priority pathogen for research and development of new antibiotics by the World Health Organization.

A goal of this study was to determine whether *A. baumannii* could catabolize ethanolamine (EA) and, if so, which enzymes were required to degrade this aminoalcohol. Inspection of the genome of this bacterium suggested that EA could be catabolized and used as a source of carbon, energy, and nitrogen. In pathogens such as *Salmonella enterica* subsp. *enterica* serovar Typhimurium strain LT2 (hereafter *S.* Typhimurium), EA catabolism plays an important role in cell fitness, survival, and infection (1–3).

Bioinformatics analysis of the *A. baumannii* genome provided a very intriguing picture of how EA may be catabolized in this bacterium. We identified homologues of some of the genes required for EA degradation in *S.* Typhimurium, where such metabolic capabilities have been studied in detail (4). The genome of *S.* Typhimurium contains a 16-gene operon (*eutSPQTDMNEJGHABCLK*) that encodes functions needed for the safe breakdown of EA inside a structure that is referred to as the Eut metabolosome (5, 6). *S.* Typhimurium controls the expression of the *eut* operon with an AraC-like protein known as EutR, which binds adenosylcobalamin (AdoCbl) and EA before it activates the expression of the *eut* operon (Fig. 1A). In contrast, the *A. baumannii* genome encodes only a putative 4-gene *eut* operon (locus tags A1S_2102, A1S_2103, A1S_2104, and A1S_2106) and a divergently transcribed regulator (*eatR* [locus tag A1S_2101]) encoding a σ^{54} enhancer binding protein (7) (Fig. 1B). Two additional genes immediately upstream and divergently transcribed from the putative regulator may also participate in the catabolism of EA. If this were the case, six functions would be needed to break down EA in *A. baumannii* (Fig. 1B; see also Fig. S1 in the supplemental material). Notably, the genome does not encode the shell proteins that comprise the *S.* Typhimurium metabolosome. This fact is important because it suggests that EA catabolism in *A. baumannii* is not contained within a metabolosome, raising the question of how this bacterium controls reactive intermediates generated during EA catabolism in the absence of such a physical structure.

The first step of EA catabolism is catalyzed by the AdoCbl-dependent EA ammonia-lyase (EAL) encoded by the *eutBC* genes (8–10) (Fig. 2). As mentioned above, in *S.* Typhimurium, this metabolic pathway occurs inside the metabolosome (6) to prevent cell damage by acetaldehyde and to sequester and concentrate the substrates, enzymes, and coenzymes needed for the efficient catabolism of EA (e.g., AdoCbl, NAD$^+$, and CoA) (11, 12). Previous studies in *S.* Typhimurium demonstrated that under certain conditions, EAL alone was sufficient for ethanolamine catabolism only when exogenous glutathione was provided to mitigate the damaging effects of acetaldehyde (6).

Figure 2 depicts two steps pertinent to the work reported here, namely, the conversion of Co(II)Cbl to AdoCbl by EutT ("AdoCbl biosynthesis" in Fig. 2) and the exchange
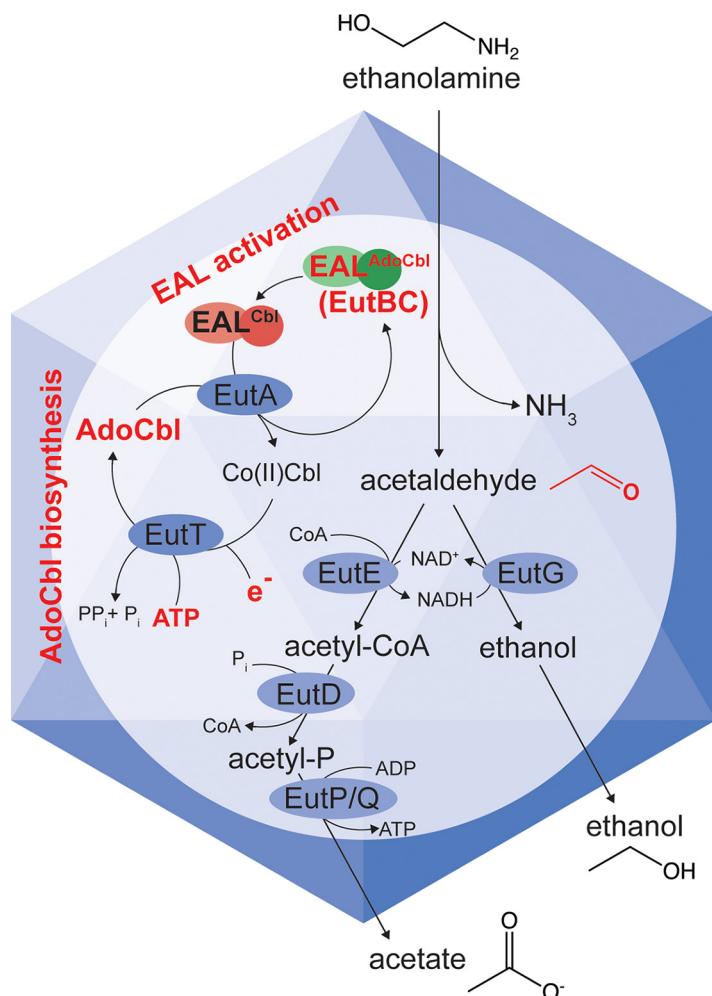
FIG 2 The *S.* Typhimurium Eut metabolosome. Indicated in red are the functions present in *A. baumannii*. The genome of this bacterium does not encode any of the shell proteins. Highlighted in red are areas of the pathway studied in this work.

of AdoCbl for Co(II)Cbl by EutA ("EAL activation" in Fig. 2). Notably, the *A. baumannii* genome lacks a EutT-type ATP:co(I)rrinoid adenosyltransferase (ACAT) (13–17) needed for the synthesis of an adenosylcobamide (AdoCba), the cofactor of the EAL enzyme. We have identified a putative PduO-type ACAT elsewhere on the chromosome (locus tag A1S_2878) (Fig. S2). PduO ACATs are the most widespread ACATs in prokaryotes, and homologues are the only type of ACATs found in humans (18–20).

The absence of most *eut* genes in *A. baumannii* suggests that this organism may have evolved a new way of breaking down EA that does not expose the cell to acetaldehyde damage. Furthermore, the lack of an identifiable EutA reactivase structural homologue presents two possibilities: either *A. baumannii* EAL (*Ab*EAL) better protects AdoCbl from inactivation than *S.* Typhimurium EAL or there is a functional homologue of the *S.* Typhimurium EutA (*Se*EutA) reactivase that is yet to be discovered in *A. baumannii*.

While the *A. baumannii* genome does not encode functions for the *de novo* synthesis of the corrin ring of AdoCba, it does encode homologues of enzymes required for the assembly of the nucleotide loop of AdoCba (Fig. 3). These genes are *cobU* (A1S_1659), *cobS* (A1S_1663), *cobT* (A1S_1660), and *cobC* (A1S_1661) (Fig. S3), and studies in other organisms have shown that their products activate the corrin ring and the nucleobase, condense the activated precursors, and dephosphorylate the last
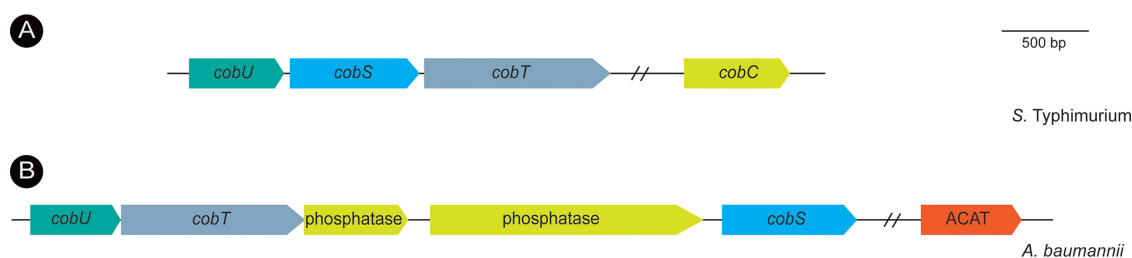
FIG 3 Organization of genes encoding nucleotide loop assembly enzymes in *S.* Typhimurium and *A. baumannii*. (A) *S.* Typhimurium enzymes have been studied in detail. (B) The *A. baumannii* genes encode hypothetical proteins whose enzymatic activities had not been described prior to this work. *cobU* encodes the bifunctional nucleotide triphosphate (NTP):Ado-cobinamide kinase (EC 2.7.1.156)–GTP:Adenosylcobinamide phosphate (AdoCbi-P) guanylyltransferase (EC 2.7.7.62), *cobT* encodes nicotinate mononucleotide:dimethylbenzimidazole phosphoribosyltransferase (EC 2.4.2.21), *cobS* encodes AdoCba 5′-P synthase (EC 2.7.8.26), and *cobC* encodes AdoCba 5′-P phosphatase (EC 3.1.3.73). ACAT is the abbreviation for ATP:co(I)rrinoid adenosyltransferase (EC 2.5.1.17).

intermediate to yield biologically active cobamides (Fig. S4) (21). Collectively, the presence of these putative functions suggested that *A. baumannii* could salvage incomplete corrinoids and convert them into biologically active coenzymes.

In this work, we (i) experimentally validate the ability of *A. baumannii* to utilize ethanolamine as a sole carbon, nitrogen, and energy source; (ii) show that the increased expression of *eutBC* is required for *A. baumannii* to utilize ethanolamine as a sole carbon source; (iii) show that *Ab*EAL is sufficient to support ethanolamine utilization in the absence of all other Eut proteins; (iv) determine that the *A. baumannii* ethanolamine ammonia-lyase *Ab*EutBC localizes to the cell membranes of *A. baumannii* and *S.* Typhimurium; (v) show that ethanolamine catabolism relies on the availability of an AdoCba and that the *A. baumannii* genome encodes the functions needed to assemble the nucleotide loop of an AdoCba from a precursor such as cobinamide; (vi) show that *A. baumannii* synthesizes a functional PduO-type ATP:Co(I)rrinoid adenosyltransferase; and (vii) show that *Ab*EutBC can utilize various adenosylcobamides and that *A. baumannii* predominantly makes cobalamin from cobinamide in the absence of exogenous base supplementation.

RESULTS

Chromosomal expression of *eutBC* allows *A. baumannii* to use ethanolamine as a sole nitrogen source but not as a carbon and energy source. To determine whether *A. baumannii* could use EA as a nitrogen source, growth was assessed in minimal medium containing M9 salts made without NH$_4$Cl but supplemented with ethanolamine as the sole source of nitrogen (Fig. 4A). To determine whether *A. baumannii* could
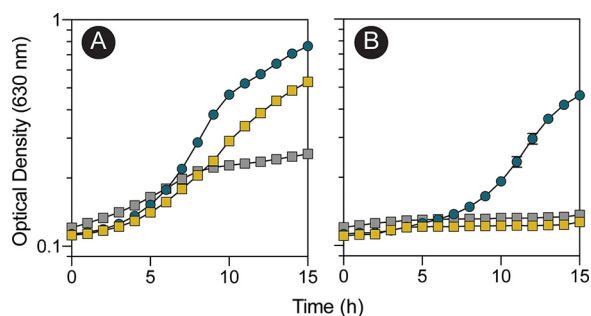
FIG 4 *A. baumannii* can use ethanolamine as a sole source of carbon or nitrogen. *A. baumannii* was grown on M9 minimal medium with ethanolamine as the sole source of nitrogen (A) or carbon and energy (B). Yellow squares, wild-type *A. baumannii* ATCC 17978; gray squares, Δ*eutBC*; blue circles, Δ*eutBC*/pAbeutBC3. For plasmid maintenance, ampicillin was added to cultures at 100 μg/mL. Experiments were performed in biological and technical triplicates. Error bars represent the standard deviations between replicates.
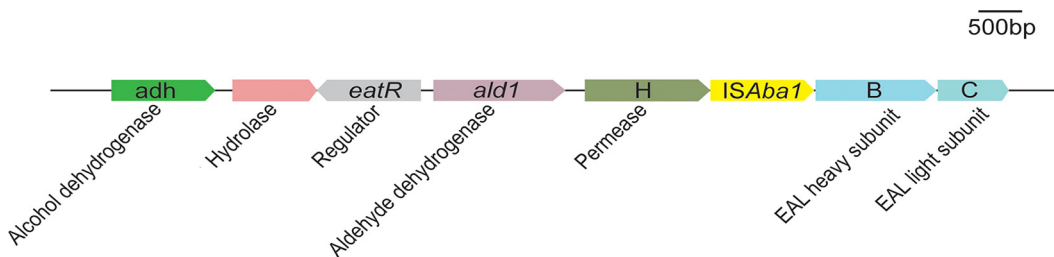
FIG 5 Spontaneous insertion of IS*Aba1* upstream of *eutBC* facilitates increased expression sufficient for growth using ethanolamine as a sole carbon source. Genes are presented at scale (see the scale bar).

use EA as a carbon and energy source, M9 minimal medium (containing NH$_4$Cl) was supplemented with ethanolamine as the sole source of carbon and energy (Fig. 4B). The growth of *A. baumannii* with ethanolamine depended on wild-type alleles of the *eutBC* genes (Fig. 4A and B, gray squares), which encode the subunits of the adenosylcobalamin (AdoCbl)-dependent EAL enzyme subunits. Chromosomal levels of *eutBC* expression were sufficient to support growth with ethanolamine as a nitrogen source (Fig. 4A, yellow squares). When *eutBC* was overexpressed in *trans*, the cultures reached a higher density (Fig. 4A, blue circles). In contrast, *A. baumannii* grew with ethanolamine as the sole source of carbon and energy in medium supplemented with cyanocobalamin (CNCbl) only when *eutBC* was overexpressed (Fig. 4B, blue circles versus yellow squares).

Spontaneous *A. baumannii* mutant strains grow robustly on ethanolamine when *eutBC* expression is driven by the IS*Aba1* element. We isolated spontaneous mutant strains of *A. baumannii* that abolished the extended lag time of the wild-type strain growing on ethanolamine as a carbon and energy source (Fig. 4B). The putative mutants were obtained after ~100 h of incubation in liquid medium at 37°C. To test the stability of the causative mutation(s), we passaged the mutant strain several times on solid and liquid rich medium devoid of ethanolamine. This strain maintained the ability to rapidly grow with ethanolamine as a carbon and energy source. These results suggested that the phenotype was the result of one or more stable mutations. To determine the nature of the mutation(s), we sequenced the genome of the mutant strain, and the analysis of the sequence revealed an insertion of the IS*Aba1* transposable element upstream of the *eutBC* genes, between the 3′ end of the *eutH* gene (which encodes a putative ethanolamine permease) and the start of *eutB* (which encodes the putative large subunit of ethanolamine ammonia-lyase) (Fig. 5; see also Fig. S5 in the supplemental material). This element was inserted immediately after the final nucleotide of *eutH*, leaving the 16-bp length upstream of *eutB* undisrupted.

Previous reports have shown that the IS*Aba1* element contains a σ^{70} promoter at the 3′ end of the gene and that this promoter is used to increase the expression of downstream genes (22). This element is frequently associated with the increased expression of antibiotic resistance genes in a clinical setting (22–26). The predicted σ^{70} sites found in IS*Aba1* are illustrated in Fig. S5.

We used the strain with the IS*Aba1* element driving the synthesis of *Ab*EutBC to determine the optimal concentrations of ethanolamine as a sole carbon source and CNCbl during growth in minimal medium (Fig. 6A and B). Strong growth was observed at 10 nM CNCbl and 75 mM ethanolamine as the sole source of carbon and energy (Fig. 6A, blue squares, and Fig. 6B, blue circles). As little as 0.5 nM CNCbl and 10 mM EA promoted robust growth when EA was used as the sole source of nitrogen by the *A. baumannii* parental strain (Fig. 6C, yellow squares, and Fig. 6D, blue circles).

Assessment of *A. baumannii* EutBC function in a heterologous host. We used well-characterized *eut* mutant strains of *S.* Typhimurium to assess the level of activity of the *Ab*EutBC enzyme in different genetic backgrounds, namely, a Δ*eutBC* strain, a Δ*eutABC* strain, or a strain carrying a deletion of the entire *eut* operon (Δ*eut*) (Fig. 7). *Ab*EutBC supported the growth of an *S.* Typhimurium Δ*eutBC* strain with EA as the sole source of nitrogen as well as *Se*EutBC did (Fig. 7A, orange squares versus green circles).
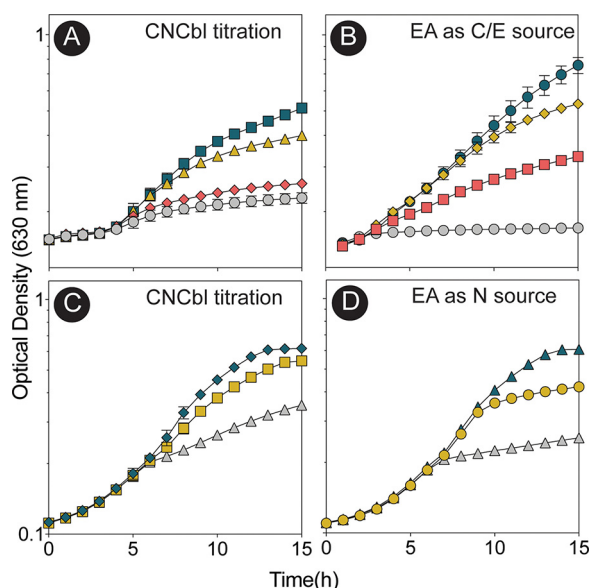
FIG 6 Analysis of cobamide and ethanolamine requirements. (Top) Cobalamin and EA requirements of the strain carrying the IS*Aba1* element during growth on EA as a sole carbon source. (A) CNCbl was provided at the following concentrations: none (gray circles), 0.5 nM (orange diamonds), 5 nM (mustard triangles), and 10 nM (blue squares). (B) EA was tested as a carbon and energy (C/E) source at the following concentrations: none (gray circles), 10 mM (orange squares), 25 mM (mustard diamonds), and 75 mM (blue circles). (Bottom) Cobalamin and EA requirements of the parental *A. baumannii* strain during growth with EA as a sole nitrogen source. (C) Titration of CNCbl at the following concentrations: none (gray triangles), 0.5 nM (mustard squares), and 5 nM (blue diamonds). (D) The following EA concentrations were tested: none (gray triangles), 1 mM (mustard circles), and 10 mM (blue triangles). In all cases, experiments were performed in biological triplicate with technical triplicates. Error bars indicate the standard deviations between replicates.

Notably, the *Ab*EutBC enzyme remained active in the absence of the *Se*EutA reactivase (Fig. 7B, green circles), while, as expected, the *Se*EutBC enzyme did not support growth in the absence of *Se*EutA (Fig. 7B, orange squares). Most intriguingly, *Ab*EutBC alone supported ethanolamine utilization in an *S.* Typhimurium strain in which the entire *eut* operon was deleted. Consistent with the need for *Se*EutA and other *eut* operon gene products, *Se*EutBC supported poor growth of the Δ*eut* strain (Fig. 7C, green circles versus orange squares). *Se*EutBC components (49.4 and 32.1 kDa, respectively) were detected at higher levels in the crude lysate (Fig. 7E, lanes 2 to 4) than *Ab*EutBC (50.6 and 30.1 kDa, respectively) (Fig. 7E, lanes 5 to 8). This was likely due to a stronger reaction to the anti-EAL antibody, as this antibody was generated against *Se*EutBC. The reduced signal observed for *Ab*EutC was likely due to protein instability under the tested conditions, as the theoretical pI of *Ab*EutC is 6.96. The loading buffer and gel stacking layer in this experiment were both pH 6.8.

Genes associated with ethanolamine utilization are cotranscribed. To test whether the putative *eut* genes were cotranscribed, primers were generated to amplify the intergenic regions between *ald1* and *eutH*, *eutH* and *eutB*, and *eutB* and *eutC* (Fig. 8A). As previously shown in *Pseudomonas aeruginosa*, all four genes were transcribed as a polycistronic mRNA and expressed from a promoter upstream of *ald1* in wild-type *A. baumannii* (Fig. 8B) (7). We used quantitative reverse transcription PCR (RT-qPCR) to determine that the evolved strain (ES) overexpresses *eutBC* (Fig. 8C). In the absence of EA, wild-type *A. baumannii* produced extremely low levels of *eutBC* transcripts (Fig. 8C, yellow striped bars). The evolved strain carrying an Is*Aba1* insertion upstream of *eutBC* grown with ethanolamine as a sole carbon source showed significant increases in *eutBC* expression (100-fold and 64-fold, respectively) compared to the parental strain, while *eutH* levels were very low in both strains and under both conditions tested. We tested the expression of the upstream *ald1* gene to determine whether this might act
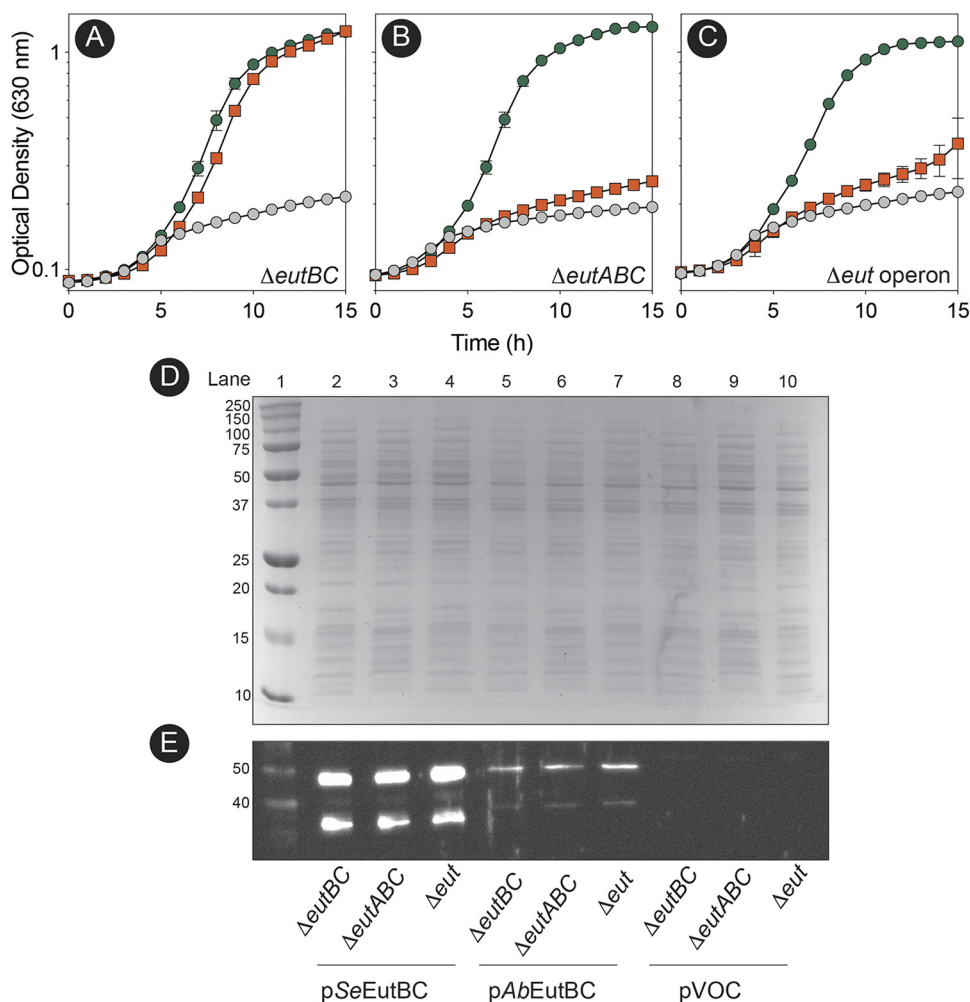
FIG 7 The *Ab*EutBC enzyme supports robust growth of *S.* Typhimurium *eut* mutants when ethanolamine is the sole source of nitrogen and does not require EutA reactivase function to remain active. (A to C) Strains were grown in nce minimal medium containing ethanolamine as the sole source of nitrogen. In all panels, the growth behaviors of strains carrying plasmid pEUT269 (*S.* Typhimurium *eutBC*$^+$) are represented by orange squares, the strain that carried plasmid pAbEUTBC1 (*A. baumannii eutBC*$^+$) is represented by green circles, and the strain that carried the empty cloning vector is represented by gray circles. The background of each strain tested is indicated at the bottom right-hand side of the panel. For plasmid maintenance, ampicillin was added to cultures at 100 μg/mL. In all cases, each strain was grown in biological and technical triplicate. Error bars indicate the standard deviations between replicates. (D) SDS-PAGE gel of crude lysates from strains used for growth analysis. Lane 1 contains molecular mass standards reported in kilodaltons. (E) Anti-EAL Western blot of crude lysates from strains used for growth analysis.

as an acetaldehyde dehydrogenase gene and aid in the management of reactive intermediates during EA catabolism. Interestingly, *ald1* was expressed at high levels in wild-type *A. baumannii* even in the absence of EA (Fig. 8D); therefore, fluctuations in gene expression in response to EA may not be detectable under the conditions used. This suggested that under some conditions, *ald1* and *eutHBC* were cotranscribed, but the expression of *ald1* may be subject to other regulatory mechanisms.

Transmission electron microscopy reveals the absence of metabolosome structures in *A. baumannii* grown with ethanolamine. We used transmission electron microscopy (TEM) and immunogold labeling to localize the *Ab*EutBC proteins within the *A. baumannii* cell. Previous reports have shown that *Se*EutBC was associated with the metabolosome (27), which can be visualized by TEM (6). No similar structures were visible in *A. baumannii* cells in the presence of EA as a sole carbon source (Fig. 9A; Fig. S6A and B). In addition, *Ab*EutBC localized primarily to the periphery of cells, with some protein apparently being interspersed throughout the cytosol. We further investigated
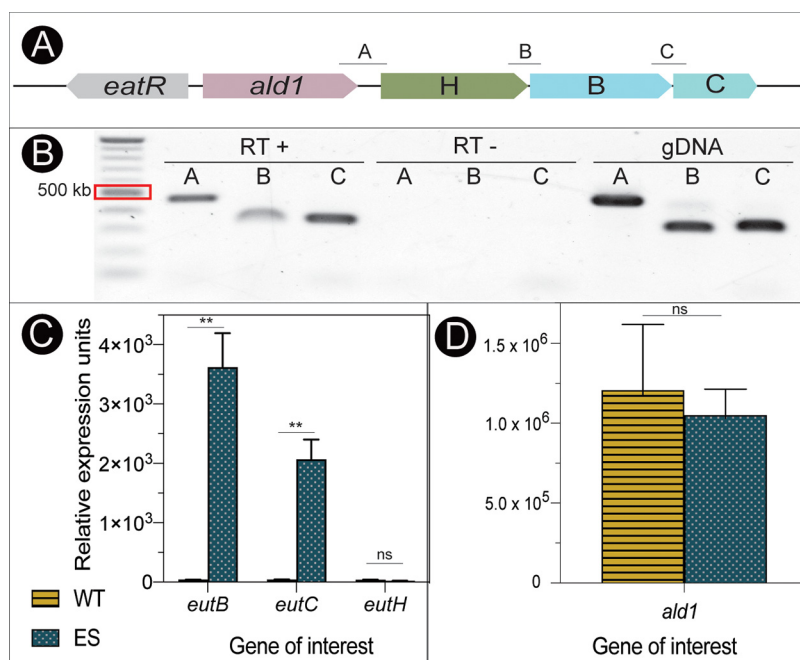
FIG 8 Expression of the putative *A. baumannii eut* genes. (A) Schematic of intergenic primers to test the putative *eut* operon. (B) Gel image of amplified products using intergenic primers and RNA extracted from *A. baumannii* incubated with (RT +) or without (RT −) reverse transcriptase or gDNA as the template. (C) RT-qPCR results of *eutB*, *eutC*, and *eutH* gene expression in wild-type (WT) *A. baumannii* grown on pyruvate (yellow stripes) or the evolved strain (ES) grown on ethanolamine as a sole carbon source (blue dots). (D) RT-qPCR results of *ald1* expression in wild-type *A. baumannii* grown on pyruvate (yellow stripes) or the evolved strain grown on ethanolamine as a sole carbon source (blue dots). **, *P* value of <0.01; ns, not significant.

localization within the cell by overexpressing *Ab*EutBC in an *S.* Typhimurium Δ*eutBC* strain (Fig. 9B; Fig. S6C and D). It is important to note that the genome of this strain of *S.* Typhimurium harbors the genes for the metabolosome shell. When expressed in the presence of the *eut* metabolosome, *Ab*EutBC did not associate with the metabolosome structure; strikingly, it was associated exclusively with the cell membrane (Fig. 9B). No EAL was detected in control samples treated with a secondary antibody only (Fig. S7).

A. baumannii synthesizes cobamides from the precursor cobinamide. The *Se*EutBC enzyme requires AdoCbl as its cofactor (28). Our bioinformatics analysis of the
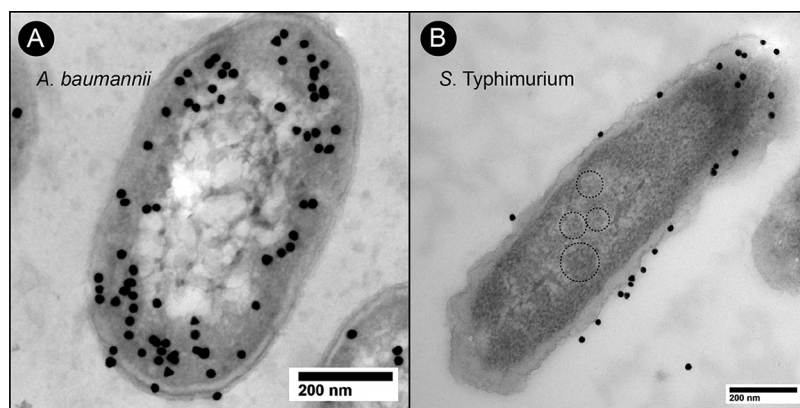
FIG 9 *A. baumannii* EutBC localizes to the cell membrane. TEM images of *A. baumannii* Δ*eutBC* (JE26441) (A) and *S.* Typhimurium Δ*eutBC* (JE26302) (B) grown on EA and expressing *Ab*EutBC in *trans* are shown. For plasmid maintenance, kanamycin (50 μg/mL) was added to *A. baumannii* cultures, and ampicillin (100 μg/mL) was added to *S.* Typhimurium cultures. Grids were labeled with a primary antibody generated against *S.* Typhimurium EutBC and a gold-conjugated secondary antibody and poststained with uranyl acetate. Metabolosomes are indicated with dotted circles.
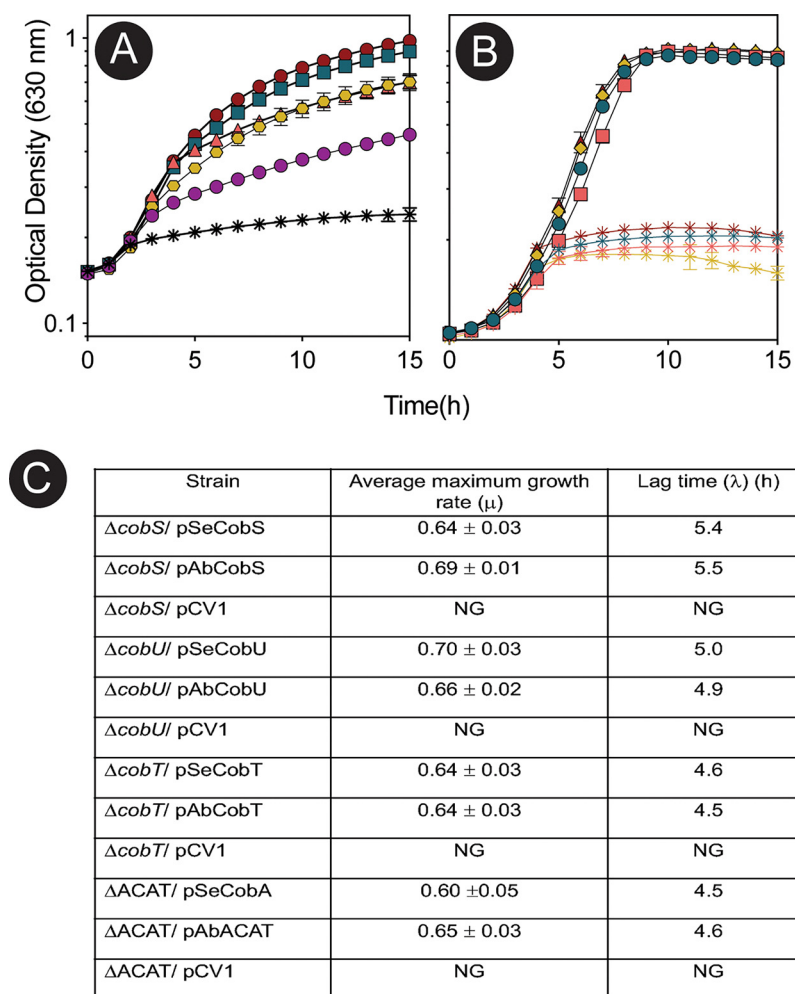
FIG 10 *A. baumannii* can salvage cobinamide to form a complete cobamide. (A) EA utilization by the *A. baumannii* evolved strain (ES) grown in minimal medium containing EA as the sole source of carbon and energy. To test the utilization of various bases, cultures were supplemented with cobalamin (red circles) or cobinamide with the addition of 5-methoxybenzimidazole (cyan squares), adenine (green triangles), 5,6-dimethylbenzimidazole (yellow hexagons), no base (purple circles), or no cobamide (gray diamonds). (B) Complementation of *A. baumannii* NLA genes in *S.* Typhimurium. Red squares, Δ*cobS*/pAbCobS; open inverted orange triangles, Δ*cobS*/vector; cyan squares, Δ*cobU*/pAbCobU; black diamonds, Δ*cobU*/vector; green triangles, Δ*cobT*/pAbCobT; blue hexagons, Δ*cobT*/vector; yellow diamonds, ΔACAT/pAbACAT; purple circles, ΔACAT/vector. Ampicillin (100 μg/mL) was added to cultures for plasmid maintenance. For each strain, the growth behavior of three separate biological replicates in technical triplicate was analyzed. Error bars represent the standard deviation between replicates. (C) Growth behavior of *S.* Typhimurium strains expressing *A. baumannii* genes. Growth rates were determined using online tools (https://scott-h-saunders.shinyapps.io/gompertz_fitting_0v2/).

A. baumannii genome indicated that this bacterium lacked the functions needed for the *de novo* synthesis of the corrin ring of cobamides but appeared to encode the function needed to adenosylate the corrin ring, i.e., to attach the adenosyl (Ado) moiety from ATP to the Co ion of the ring, and the functions required for the assembly of the nucleotide loop (29).

The formation of a complete coenzyme from the precursor cobinamide requires the nucleotide loop assembly (NLA) pathway (Fig. S4). Under the conditions tested, *A. baumannii* salvaged the precursor cobinamide and other nitrogenous bases to form a functional coenzyme and facilitate growth with EA, demonstrating that NLA pathway enzymes were functional (Fig. 10A). We also tested the activity of NLA enzymes using heterologous expression in a MetH-dependent *S.* Typhimurium strain. The *A. baumannii* NLA enzymes CobU, CobS, and CobT compensated for the absence of the *cobU*,

cobS, and *cobT* genes of *S*. Typhimurium (Fig. 10B and C). Furthermore, the *A. baumannii pduO*-type ACAT supported EA metabolism in an *S*. Typhimurium ACAT-null strain. The NLA enzymes CobU and CobS require adenosylated substrates (30, 31); thus, salvaging of the precursor cobinamide depended on the function of the *A. baumannii* ACAT under these conditions (Fig. 10B and C). These results demonstrated that *A. baumannii* NLA and ACAT homologues were functional.

Cobalamin is produced by *A. baumannii* in the absence of nucleobase supplementation. Prokaryotes can utilize numerous nucleobases to yield a functional coenzyme (32). As shown in Fig. 10A, various bases can be used by *A. baumannii* to form a functional coenzyme. Salvaging was performed in the absence of exogenous nucleobases; however, this led to diminished growth (Fig. 10A, purple circles). To determine the identity of this cobamide produced by *A. baumannii* in the absence of exogenous nucleobases, we extracted cobamides and separated them using reverse-phase high-performance liquid chromatography (RP-HPLC) as described in Materials and Methods. A compound eluted off the column 33 min after sample injection. The retention time was equal to the retention time of commercially available CNCbl (Fig. S8A and B). This peak was collected, cleaned, and analyzed using matrix-assisted laser desorption ionization–time of flight (MALDI-TOF) mass spectrometry, confirming that cobalamin, the cobamide containing 5,6-dimethylbenzimidazole (DMB) as its nucleobase, was the cobamide synthesized by *A. baumannii* in the absence of exogenous nucleobases (Fig. S8C).

DISCUSSION

***A. baumannii* catabolizes ethanolamine as a source of carbon and nitrogen.** Based on the data presented here, we surmised that the wild-type strain of *A. baumannii* used in this work synthesizes insufficient *Ab*EutBC to support growth with EA as the sole carbon and energy source. It is possible, however, that in its natural environment, *A. baumannii* uses EA mainly as a source of nitrogen, and for that purpose, enough EAL is produced from chromosomal expression levels. Our data show that *A. baumannii* can use the IS*Aba1* element to increase the expression of *eutBC* if selective pressure for the use of ethanolamine as a carbon and energy source arises in its environment. Previous studies have identified IS*Aba1* upstream of antibiotic resistance genes in patient samples, suggesting that this is a clinically relevant adaptive mechanism used by this organism during human infection (23). The insertion of an IS*Aba1* element does not affect the expression of the upstream *eutH* and *ald1* genes. The low level of *eutH*, even in the presence of EA, suggests that, under the conditions tested, active transport is not required and that sufficient EA diffuses across the membrane into the cell. We have shown that the requirements for both cobamide and EA concentrations are lower in *A. baumannii* than in *S*. Typhimurium. This reduced need may reflect the faster access of enzymes to these molecules due to the lack of restriction by the metabolosome.

***Ab*EAL is sufficient to support ethanolamine metabolism in the absence of a metabolosome or EAL reactivase.** We did not identify genes encoding homologues of metabolosome shell proteins in the *A. baumannii* genome, suggesting to us that *A. baumannii* may be able to perform this metabolism without containment in a microcompartment. The N terminus of *Se*EutC contains a signal sequence involved in localization to the microcompartment (33). Consistent with the lack of any genes encoding microcompartment shell proteins, the *Ab*EutC sequence also lacks any predicted N-terminal signal sequence (see Fig. S1D in the supplemental material). We showed here that *Ab*EAL does not require a reactivase; furthermore, *Ab*EAL alone can support EA utilization in the absence of the entire *S*. Typhimurium *eut* operon. This suggests that either the *Ab*EAL enzyme directly quenches the acetaldehyde generated from EA or *A. baumannii* reduces cellular damage caused by acetaldehyde using an alternative mechanism. The mechanism by which *Ab*EAL functions in the absence of a physical metabolosome is intriguing. Using TEM, we showed that *A. baumannii* does not form metabolosomes and that the enzyme does not associate with metabolosomes when expressed in *S*. Typhimurium (Fig. 9). Based on these data, we surmise that the *Ab*EAL

enzyme acts independently of other Eut components in *S.* Typhimurium. The membrane association of *Ab*EAL was more pronounced when expressed in *S.* Typhimurium. It is possible that this is due to the association of *Ab*EAL with other B_{12}-related enzymes not found in *A. baumannii*. We hypothesize that in *A. baumannii*, other enzymes, such as the cotranscribed aldehyde dehydrogenase, associate with *Ab*EAL to facilitate the swift quenching of reactive molecules and prevent cellular damage. To our knowledge, this is the first report of ethanolamine metabolism occurring in an organism that does not form a metabolosome.

Multiple cobamides can be formed by the *A. baumannii* salvaging pathway and used as a coenzyme by *Ab*EAL. *A. baumannii* carries the genes for nucleotide loop assembly as well as a functional PduO-type ACAT. Due to the apparent absence of other genes related to propanediol metabolism, we instead refer to this protein as a general ACAT (AcaT). The unique organization of these genes in *A. baumannii* is notable, as the *cobUST* genes are typically organized immediately adjacent to each other. We have shown experimental evidence that the *cobU*, *cobT*, and *cobS* gene products facilitate the use of various nucleobases to form the nucleotide loop and that the resulting cobamides function as coenzymes for *Ab*EAL. This is consistent with a previous report in which *Se*EAL was shown to also use pseudocobalamin (34). Structural studies would provide insight into the ability of this enzyme complex to utilize multiple cobamide coenzymes.

Ethanolamine metabolism and pathogenesis. Understanding the metabolic capabilities of *A. baumannii* is of great interest as we attempt to combat antimicrobial resistance. EA has been shown to play a role in the environmental sensing and pathogenesis of *S.* Typhimurium and *Escherichia coli* (3, 35, 36). Although *A. baumannii* is not generally associated with gastrointestinal disease or part of a normal gut microbiome, it has been found to inhabit the digestive tract of long-term-ICU (intensive care unit) patients (37), indicating that the intestine may be a reservoir for this nosocomial pathogen. EA breakdown may be an important metabolic capability for *A. baumannii* during the course of colonization or infection, and if so, the enzymes studied here could serve as effective therapeutic targets.

MATERIALS AND METHODS

Bacterial strains and growth conditions. The *S.* Typhimurium and *A. baumannii* strains used in this study are listed in Table S1 in the supplemental material. All *A. baumannii* strains used were derivatives of *A. baumannii* ATCC 17978. All *S.* Typhimurium strains used were derivatives of *S. enterica* subsp. *enterica* serovar Typhimurium strain LT2. *E. coli* DH5α was used for plasmid construction. All cultures were grown at 37°C. *A. baumannii* was grown in lysogeny broth (LB) (38, 39) or M9 minimal medium (40). To test EA as a carbon source, M9 minimal medium was supplemented with $MgSO_4$ (1 mM), $CaCl_2$ (10 μM), EA-HCl (90 mM, unless otherwise noted), LB (1%, vol/vol), and cyanocobalamin (CNCbl) (100 nM, unless otherwise noted). To test EA as a nitrogen source, *A. baumannii* was grown in nitrogen-free M9 salts supplemented with $MgSO_4$ (1 mM), $CaCl_2$ (10 μM), sodium pyruvate (20 mM), CNCbl (10 nM, unless otherwise noted), and EA-HCl (30 mM, unless otherwise noted). *S.* Typhimurium strains were grown on nutrient broth (NB; Difco) or no-carbon essential (NCE) minimal medium (41); *E. coli* was grown in LB. When antibiotics were used, their concentrations were indicated for each experiment. Unless otherwise noted, isopropyl β-D-1-thiogalactopyranoside (IPTG) was used at 1 mM, and L-(+)-arabinose was used as an inducer of gene expression at 0.5 mM. Unless otherwise specified, all chemicals were purchased from Sigma-Aldrich Chemical Company.

Construction of *A. baumannii* deletion strains. Deletions were constructed as described previously (42, 43). *A. baumannii* harboring plasmid pRecABtet was transformed with a fragment containing flanking regions of the gene of interest fused to the kanamycin (Km) resistance gene from plasmid pKD4 by electroporation. Cells were recovered using superoptimal broth with catabolite (SOC) repression medium (tryptone [20 g/L, wt/vol], yeast extract [5 g/L], NaCl [0.5 g/L], glucose [20 mM]) at 37°C with shaking at 220 rpm for 2 to 4 h. Following incubation, cells were plated onto LB (Difco) agar plates containing Km (25 μg/mL) and IPTG (2 mM). Kanamycin-resistant (Km^r) transformants were patched onto plates containing tetracycline (Tc) (10 μg/mL), and tetracycline-sensitive (Tc^s) Km^r colonies were analyzed further. To resolve the kanamycin cassette, plasmid pFLPtet was moved into the strains by electroporation. Cells were recovered with SOC medium (2 mL) for 2 to 4 h at 37°C with shaking at 220 rpm and plated onto LB agar containing tetracycline (10 μg/mL). Cells were streaked for isolation onto plates containing tetracycline (10 μg/mL) and IPTG (2 mM) to induce the expression of *flp*. Isolated colonies were streaked onto LB and then patched onto LB agar containing kanamycin (30 μg/mL) or tetracycline (10 μg/mL). We isolated genomic DNA (gDNA) from Tc^s Km^s colonies as described previously (42), followed by PCR amplification and DNA sequencing to verify the disruption of the gene of interest and the loss of the Km resistance cassette.

Plasmid construction. Plasmids used in this study are listed in Table S1. Primers used for the construction of strains, the construction of complementation plasmids, and PCR analysis are listed in Table S2. To test complementation in *S.* Typhimurium, each gene of interest from *A. baumannii* was cloned into cloning vector pCV1 (44) using BspQI restriction sites and electroporated into *E. coli* DH5α. Plasmids were miniprepped using a Wizard Plus SV Minipreps DNA purification system (VWR) and sequenced to verify each insert. Positive plasmids were electroporated into an *S.* Typhimurium strain carrying a deletion of the homologous gene. Cells containing the plasmid were selected for by the addition of ampicillin (100 μg/mL) to the growth medium.

Complementation studies in *A. baumannii* were performed as described previously (45). *A. baumannii eutBC* was inserted into pMMB67EH using EcoRI and SalI (Thermo Fisher) restriction digests, and ligation was then performed using T4 DNA ligase (Thermo Fisher) according to the manufacturer's instructions. Chemically competent *E. coli* DH5α was transformed and plated onto Tc (10 μg/mL). Selected colonies were miniprepped and sequenced to verify the insertion. Verified plasmids were used to transform electrocompetent *A. baumannii* $\Delta eutBC$ as described above, and cells were recovered in SOC medium for 2 to 4 h and plated onto LB agar containing tetracycline.

Analysis of EA catabolism in *A. baumannii*. *A. baumannii* strains were grown in LB overnight and subcultured (5%, vol/vol) into M9 minimal medium or nitrogen-free M9 minimal medium. Growth analyses were performed using a 96-well microtiter dish (Falcon) with 200 μL per well, cultures were incubated at 37°C with shaking, and increases in cell density were monitored at 630 nm for 24 h. Each growth analysis consisted of three biological replicates in technical triplicate. Concentrations of CNCbl or ethanolamine were changed where indicated to assess the minimal requirements of *A. baumannii* for these nutrients.

Complementation studies in *S.* Typhimurium. The heterologous expression of *A. baumannii* genes was performed in *S.* Typhimurium to test EAL, NLA, and ACAT functions. NB was inoculated with a single colony, and the colony was grown overnight at 37°C. The following day, 1% (vol/vol) of overnight culture (~16 h old) was transferred into minimal medium in a 96-well microtiter plate. *S.* Typhimurium growth experiments were performed in NCE minimal medium (41) containing Wolfe's trace minerals (46), MgSO$_4$ (1 mM), glycerol (22 mM), and ampicillin (100 μg/mL). Cobamide precursor salvaging was performed by assessing growth with the addition of dicyanocobinamide [(CN)$_2$Cbi] and 5,6-dimethylbenzimidazole (DMB) (150 μM). Gene expression was induced with L-(+)-arabinose (0.5 μM). The growth of cultures in microtiter plates was monitored every hour at 630 nm during incubation with shaking at 37°C in a BioTek Elx808 microplate reader. To test the functionality of the *A. baumannii eutBC* gene products, minimal medium containing nocarbon nonessential NCE medium (47) with ethanolamine (30 mM) provided as the sole source of nitrogen was used. In each case, growth analysis was performed in a BioTek Elx808 microplate reader with three biological replicates in technical triplicate.

Sequencing of *A. baumannii* genomes. Strains of *A. baumannii* able to grow on ethanolamine as the sole source of carbon and energy were grown overnight in LB (10 mL) at 37°C with shaking at 180 rpm. Cells were harvested by centrifugation at 3,000 $\times$ g using a tabletop Eppendorf 5810R centrifuge for 30 min at room temperature. Genomic DNA was isolated using a blood and cell culture DNA midi kit and a genomic DNA buffer set (Qiagen) according to the manufacturer's protocol for the preparation of Gram-negative samples. The quality of genomic DNA was measured using an Invitrogen Qubit model 4 fluorometer, and only samples containing >10% (wt/vol) double-stranded DNA were used for whole-genome sequencing (WGS). DNA-end repair was performed using NEBNext FFPE (formalin-fixed, paraffin-embedded) DNA repair mix and NEBNext Ultra II end repair (New England BioLabs [NEB]) according to the manufacturer's instructions. The repair reaction was allowed to proceed for 30 min at 20°C and 30 min at 65°C. DNA was isolated by mixing with AMPure XP beads, washing with 70% (vol/vol) ethanol, and eluting off beads with Ambion nuclease-free water. The eluate containing end-repaired DNA was quantified using a Qubit fluorometer. Barcodes were attached using NEB blunt/TA ligase and master mix (New England BioLabs) according to the manufacturer's instructions, and the mixture was incubated at 25°C for 15 min. DNA was purified from the reaction mix using AMPure beads according to the manufacturer's instructions and eluted in 25 μL nuclease-free water. Barcoded DNA was quantified using a Qubit fluorometer. Equimolar amounts of barcoded samples were pooled to a total of 1,050 ng in 65 μL. Adapters were attached to barcoded DNA using adapter mix, NEBNext ligation buffer, and NEBNext quick T4 DNA ligase (New England BioLabs), and the mixture was incubated at 20°C for 15 min. Following incubation, DNA was isolated from the reaction mixture using AMPure XP beads as described above. Beads were washed with long-fragment buffer (Nanopore) twice before elution with elution buffer (Nanopore). The final concentration of the library was quantified using a Qubit fluorometer. Libraries were loaded into an R10.3 flow cell on a MinION Mk1C system (Nanopore Technologies).

Antibody preparation. Purified *S.* Typhimurium EAL was provided to Envigo for the production of rabbit polyclonal antibodies. Antiserum was precleared against JE8094 ($\Delta eutBC$). Cells were grown at 37°C with shaking at 180 rpm in minimal NCE medium containing ribose (20 mM), EA (30 mM), and CNCbl (200 nM) to an optical density at 600 nm (OD$_{600}$) of ~1.0. Cells were incubated on ice for 15 min and then harvested by centrifugation at 2,000 $\times$ g for 15 min in a 5810 R centrifuge (Eppendorf). Cells were resuspended in 100 μL Tris-HCl buffer (50 mM [pH 7.5] at 4°C) containing SDS (2%, wt/vol). To lyse cells, the suspension was boiled for 5 min and then incubated on ice for 10 min. The solution was brought to a final volume of 1 mL with Tris-HCl buffer (50 mM [pH 7.5] at 4°C). Antiserum was added at a 1:100 dilution, and the mixture was incubated at 4°C for 36 h. Precleared antibody was obtained by centrifugation at 16,000 $\times$ g for 10 min and removal of the supernatant. Precleared antibody was flash-frozen in liquid N$_2$ and stored at −80°C until use.

Western blotting. *S.* Typhimurium strains were grown in NCE or no-carbon or no-nitrogen (NCN) medium containing EA (30 mM) as the sole source of nitrogen. Each medium was supplemented with Wolfe's trace minerals, $MgSO_4$ (1 mM), glycerol (22 mM), CNCbl (150 nM), ampicillin (100 μg/mL), and L-(+)-arabinose (0.5 μM). Cultures were inoculated with LB (2%, wt/vol) and grown overnight with shaking at 180 rpm at 37°C to an OD_{600} of 0.45 to 0.65. Cells were harvested using a 5810 R centrifuge (Eppendorf) at 2,220 × g for 15 min and stored at −80°C. Cells were resuspended in 1 mL sterile phosphate-buffered saline (PBS) (10 mM sodium phosphate [pH 7.4], 0.9% [wt/vol] NaCl) and centrifuged at 4,000 × g for 10 min in a 5415 D centrifuge (Eppendorf) at 4°C. Cell pellets were resuspended in bacterial protein extraction reagent (B-PER) (300 μL; Thermo Fisher) and vortexed for 1 min to lyse cells. The protein concentration in the crude lysate was quantified using Bradford protein assay dye (Bio-Rad Laboratories) according to the manufacturer's instructions. Bovine gamma globulin (Thermo Fisher) was used to generate a standard curve. Cell lysates were diluted to 500 ng/μL in PBS and incubated with loading buffer (Tris [pH 6.8] [300 mM], glycerol [60%, vol/vol], EDTA [12 mM], 2-mercaptoethanol [0.85 M], and bromophenol blue [0.05%, wt/vol]) for 5 min at 95°C. The crude lysate was loaded in duplicate onto a 15% (wt/vol) SDS-PAGE gel (48). Gels were loaded with Precision-Plus protein standards (Bio-Rad Laboratories) or a SuperSignal molecular weight protein ladder (Thermo Fisher). Gels intended for Coomassie staining were loaded with 5 μg of the crude lysate; gels intended for Western blotting were loaded with 5 μg for strains complemented with *Ab*EutBC or vector-only control (VOC) and 1.25 μg for strains complemented with *Se*EutBC. A constant voltage of 200 V was applied to gels for approximately 35 min. Gels loaded with Precision-Plus protein standards were stained with brilliant blue R dye to visualize proteins. Gels loaded with the SuperSignal molecular weight protein ladder were transferred to a polyvinylidene difluoride (PVDF) membrane using a Trans-Blot Turbo system (Bio-Rad Laboratories). Following transfer, the membrane was incubated in blocking buffer composed of 0.5% (wt/vol) nonfat milk in PBST (phosphate-buffered saline [pH 7.4] containing 0.1% [vol/vol] Tween 20 [Millipore Sigma]) for 1 h at room temperature on an advanced digital shaker (VWR). The primary antibody generated against *S.* Typhimurium EAL was diluted 1:2,000 in blocking buffer, and the membrane was incubated in this solution at 4°C overnight on a tabletop shaker. The following morning, the membrane was washed three times with PBST. The membrane was incubated in PBST containing a goat anti-rabbit IgG–horseradish peroxidase conjugate (1:20,000; Invitrogen) for 1 h at room temperature on a tabletop shaker. The membrane was washed three times with PBST, incubated with SuperSignal West Pico Plus chemiluminescent substrate (Thermo Fisher) for 10 min at room temperature, and imaged using a UVP ChemStudio system (Analytik Jena) with an exposure time of 5 s.

RNA isolation. RNA was isolated as described previously (49). A culture grown overnight in LB medium inoculated with a single colony was subcultured (2.5%, vol/vol) in 10 mL minimal medium. Cultures grown for RT-qPCR analyses were grown in M9 minimal medium containing either ethanolamine (90 mM) or pyruvate (20 mM) as a sole carbon and energy source. For cultures used in experiments aimed at determining whether the *A. baumannii* putative *eut* genes were cotranscribed, wild-type *A. baumannii* (JE25551) was grown in no-nitrogen M9 minimal medium supplemented with 30 mM ethanolamine and 20 mM pyruvate. In all cases, cultures were incubated with shaking (200 rpm) at 37°C to an OD_{600} of 0.4 with 0.5 and harvested using a 5810 R centrifuge (Eppendorf) at 3,220 × g for 10 min. The supernatant was removed, and cells were stored at −80°C until they were processed. Cell pellets were lysed by resuspending the cells in boil solution (EDTA [18 mM], SDS [0.025%, vol/vol], 2-mercaptoethanol [1%, vol/vol], formamide [95%, vol/vol], RNase-free water brought to a final volume of 1 ml and heating the suspension at 95°C for 7 min. The cell suspension was centrifuged at 16,000 × g for 5 min at room temperature, and 100 μL of the supernatant was removed into a new tube. RNase-free water (400 μL) was added to dilute the culture, and sodium acetate was added to a final concentration of 0.3 M. Ice-cold ethanol (100%) was added (1,650 μL), and samples were vortexed briefly to mix and then incubated at −80°C overnight. Samples were centrifuged for 30 min at 16,000 × g at 4°C, and the supernatant was discarded. The remaining pellet was washed with 300 μL of ice-cold 70% ethanol and centrifuged at 8,000 × g for 5 min at 4°C. The supernatant was discarded, and the pellet was allowed to air dry. RNA pellets were resuspended in 100 μL RNase-free water and centrifuged for 1 min at 16,000 × g to remove any insoluble contaminants, and 90 μL was transferred into a new tube. A DNA digest was performed using the rigorous DNase treatment for Turbo DNase according to the manufacturer's instructions (Thermo Fisher). Following DNase treatment and inactivation, samples were centrifuged at 10,000 × g for 1.5 min, and 90 μL was transferred into a new tube. A second sodium acetate-ethanol precipitation step was performed as described above. RNA yield and quality were analyzed using a Qubit 4 fluorometer using the RNA broad range (BR) assay kit and the RNA IQ assay kit, respectively (Invitrogen). Samples with an RNA IQ value of 6 or higher were used for RT-qPCR experiments.

cDNA synthesis and RT-qPCR. RNA to be used as the cDNA template was diluted to a final concentration of 12.5 ng/μL, and cDNA was synthesized using an iScript cDNA synthesis kit (Bio-Rad) according to the manufacturer's protocol. cDNA was diluted to 2.5 ng/μL when used for RT-qPCR experiments. RT-qPCRs were performed in a 96-well plate. In each well, 20 μL of reaction mix containing 10 mL Fast SYBR green master mix (Life Technologies), gene-specific primers (500 nM), and cDNA (10 ng) was added. Gene-specific primers were designed using Primer3 software. The *A. baumannii* 16S rRNA gene was used as an internal control. RT-qPCRs were run using a 7500 Fast real-time PCR system (Applied Biosystems). Three biological replicates each in technical triplicate were analyzed for each strain. The cycle threshold (C_T) was normalized against 16S values, and these values were transformed using the formula 2(e − ΔC_T)/10^{-6} and reported as arbitrary expression units (EU). The mean EU from each biological replicate was used to calculate the standard error in Prism software v9 (GraphPad). Statistical significance was determined using Welch's t test in Prism software v9 (GraphPad).

Operon PCR. Intergenic primers were generated to amplify the regions between genes within the putative operon. Five microliters of the iScript reaction product with reverse transcriptase (+RT) or

without reverse transcriptase (−RT) was added to each reaction mixture. gDNA was diluted to 12.5 ng/μL, and 5 μL was added to each control reaction mixture. PCR was performed using GoTaq green master mix (Promega) according to the manufacturer's instructions. Products were analyzed on a 1% (wt/vol) agarose DNA gel.

Cell preparation for transmission electron microscopy. *A. baumannii* was grown in M9 minimal medium containing EA as a sole carbon source. *S.* Typhimurium was grown in NCN medium supplemented with glycerol (22 mM) and EA (30 mM). In both cases, cultures were harvested at an OD_{600} of ∼0.6 in a 5810 R centrifuge (Eppendorf) at 3,220 × g for 10 min. Cell pellets were resuspended in Sorensen's phosphate buffer (0.1 M sodium phosphate [pH 7.4]) containing 4% paraformaldehyde and 0.2% glutaraldehyde and incubated at room temperature for 15 min. Fixed cells were centrifuged at 6,000 × g for 2 min. The supernatant was removed, and cells were washed twice in Sorensen's phosphate buffer. Cells were enrobed in melted, 60°C Noble agar (4% in Sorensen's buffer [pH 7.4]) and cut into 2-mm blocks for dehydration.

Samples were dehydrated by treatment with the following steps: 50% ethanol for 15 min, 70% ethanol for 15 min, and 80% ethanol for 10 min. The sample at each step was incubated on a slow rotator set at a 45° angle at room temperature. Cells were incubated with a mixture of LR white resin (London Resin Company, Ltd.) and 80% ethanol (2:1, vol/vol) for 1 h at room temperature. Cells were then incubated with LR white resin (100%) three times for 1 h each. Each incubation was performed at room temperature on a slow rotator set at a 45° angle. Cells were embedded in LR white resin in gelatin capsules and incubated at 50°C for 14 to 16 h. Sections of 30 to 50 nm were cut using a DiaTOME Ultra diamond knife mounted on an RMC-MT-X microtome. Sections were placed onto gold grids coated with Formvar and carbon until immunogold labeling was performed.

Grids were incubated top-down on a 25-μL drop of blocking buffer containing 20 mM Tris (pH 7.4), 150 mM NaCl, and 1% (wt/vol) bovine serum albumin (BSA) for 10 min and then washed by repeated dipping in a beaker containing 10 mL blocking buffer for 1 min. Grids were incubated top-down on a 25-μL drop of blocking buffer containing the primary antibody (rabbit polyclonal antibody generated against *S.* Typhimurium EAL) diluted to 1:50 overnight at room temperature. Grids were washed by dipping in a beaker containing 10 mL blocking buffer for 1 min and then incubated top-down on a 25-μL drop of blocking buffer for 15 min. Grids were then transferred top-down to a 25-μL drop of goat anti-rabbit IgG-gold antibody (Millipore Sigma) and incubated for 1 h at room temperature. A final wash was performed by dipping repeatedly in a beaker containing 10 mL blocking buffer for 0.5 min and then dipping repeatedly in a beaker containing 10 mL water for 0.5 min. Where indicated, grids were poststained by incubating them on a droplet of filtered 4% aqueous uranyl acetate for 20 min, washed thoroughly by dipping them into a beaker of deionized (DI) H_2O 30 times, and then incubated on a drop of filtered DI H_2O for 1 min. Negative controls were treated exclusively with secondary antibody. Imaging was performed using a JEOL 1011 transmission electron microscope (JEOL USA, Peabody, MA).

Cobamide extraction and identification. The isolation and identification of cobamides were performed as described previously (32). Briefly, 100 mL of M9 minimal medium containing ethanolamine (90 mM) as the sole source of carbon and energy and cobinamide (100 nM) was inoculated with 2.5% (vol/vol) of an LB liquid culture, and the culture was grown overnight at 37°C with shaking at 180 rpm. The following morning, cultures were harvested using a 5810 R centrifuge (Eppendorf) at 3,220 × g for 20 min. The cell pellet was resuspended in 10 mL buffer A (50 mM KH_2PO_4 [pH 6.5], 5 mM KCN) with 20 mL methanol and then incubated at 65°C for 2 h with shaking (220 rpm). Cell debris was removed by centrifugation at 30,000 × g in an Avanti JP20-XVI centrifuge equipped with a JA-25.50 rotor for 1 h. A SepPak C_{18} Plus cartridge (360 mg sorbent per cartridge, 55- to 105-μm particle size; Waters) was activated with methanol (10 mL) and water (10 mL). The supernatant was diluted 1:5 in water and passed over the activated SepPak cartridge. Cobamides bound to the SepPak cartridge were washed with water (20 mL) and eluted using methanol (100% [vol/vol]; 1.5 mL). Cobamides were dried overnight in a VacFuge Plus instrument (Eppendorf) and resuspended in buffer A (200 mL). KCN was added to a final concentration of 25 mM, and the mixture was incubated for 10 min in a sand bath kept at 90°C. Cobamides were then passed over a Spin-X centrifuge tube filter (Corning) for 5 min at 13,000 × g. Cleaned reaction mixtures were separated by RP-HPLC on a Shimadzu Prominence Ultra Fast Liquid Chromatography (UFLC) SPD-M30A instrument equipped with a Synergi 4μ Hydro-RP 80Å 150- by 4.6-mm column. The following method was used to separate cobamides. The column was equilibrated with 97% mobile phase A (MP A) (KH_2PO_4 [0.1 M] [pH 6.5], KCN [10 mM])–3% mobile phase B (MP B) (KH_2PO_4 [0.1 M] [pH 8], KCN [10 mM]-acetonitrile in a 1:1 ratio). Sample injection was followed by a 5-min linear gradient to 75% MP A–25% MP B, a 15-min linear gradient to 65% MP A–35% MP B, a 5-min isocratic step at 65% MP A–35% MP B, and a 2.5-min linear gradient to 100% MP B, concluding with a 5-min isocratic step at 100% MP B. Cobamides were identified by measuring the absorbance at 367 nm. Fractions containing cobamides were collected, desalted using a SepPak C_{18} cartridge, and dried overnight in a VacFuge Plus instrument. Cobamide fractions were resuspended in sterile water and sent for MALDI-TOF mass spectrometry analysis.

SUPPLEMENTAL MATERIAL

Supplemental material is available online only.

FIG S1, PDF file, 1.3 MB.

FIG S2, PDF file, 0.5 MB.

FIG S3, PDF file, 0.8 MB.

FIG S4, PDF file, 2 MB.
FIG S5, PDF file, 0.2 MB.
FIG S6, JPG file, 0.5 MB.
FIG S7, PDF file, 1 MB.
FIG S8, PDF file, 0.1 MB.
TABLE S1, PDF file, 0.1 MB.
TABLE S2, PDF file, 0.03 MB.

REFERENCES

1. Winter SE, Thiennimitr P, Winter MG, Butler BP, Huseby DL, Crawford RW, Russell JM, Bevins CL, Adams LG, Tsolis RM, Roth JR, Baumler AJ. 2010. Gut inflammation provides a respiratory electron acceptor for *Salmonella*. Nature 467:426–429. https://doi.org/10.1038/nature09415.

2. Baumler AJ, Winter SE, Thiennimitr P, Casadesus J. 2011. Intestinal and chronic infections: *Salmonella* lifestyles in hostile environments. Environ Microbiol Rep 3:508–517. https://doi.org/10.1111/j.1758-2229.2011.00242.x.

3. Anderson CJ, Clark DE, Adli M, Kendall MM. 2015. Ethanolamine signaling promotes *Salmonella* niche recognition and adaptation during infection. PLoS Pathog 11:e1005278. https://doi.org/10.1371/journal.ppat.1005278.

4. Kaval KG, Garsin DA. 2018. Ethanolamine utilization in bacteria. mBio 9: e00066-18. https://doi.org/10.1128/mBio.00066-18.

5. Kofoid E, Rappleye C, Stojiljkovic I, Roth J. 1999. The 17-gene ethanolamine (*eut*) operon of *Salmonella typhimurium* encodes five homologues of carboxysome shell proteins. J Bacteriol 181:5317–5329. https://doi.org/10.1128/JB.181.17.5317-5329.1999.

6. Brinsmade SR, Paldon T, Escalante-Semerena JC. 2005. Minimal functions and physiological conditions required for growth of *Salmonella enterica* on ethanolamine in the absence of the metabolosome. J Bacteriol 187: 8039–8046. https://doi.org/10.1128/JB.187.23.8039-8046.2005.

7. Lundgren BR, Sarwar Z, Pinto A, Ganley JG, Nomura CT. 2016. Ethanolamine catabolism in *Pseudomonas aeruginosa* PAO1 is regulated by the enhancer-binding protein EatR (PA4021) and the alternative sigma factor RpoN. J Bacteriol 198:2318–2329. https://doi.org/10.1128/JB.00357-16.

8. Roof DM, Roth JR. 1989. Functions required for vitamin B$_{12}$-dependent ethanolamine utilization in *Salmonella typhimurium*. J Bacteriol 171:3316–3323. https://doi.org/10.1128/jb.171.6.3316-3323.1989.

9. Chang GW, Chang JT. 1975. Evidence for the B12-dependent enzyme ethanolamine deaminase in *Salmonella*. Nature 254:150–151. https://doi.org/10.1038/254150a0.

10. Faust LR, Connor JA, Roof DM, Hoch JA, Babior BM. 1990. Cloning, sequencing, and expression of the genes encoding the adenosylcobalamin-dependent ethanolamine ammonia-lyase of *Salmonella typhimurium*. J Biol Chem 265:12462–12466. https://doi.org/10.1016/S0021-9258(19)38368-1.

11. Costa FG, Deery E, Warren M, Escalante-Semerena JC. 2020. Insights into the biosynthesis of cobamides and their use, p 364–394. *In* Liu H-W, Begley TP (ed), Comprehensive natural products III: chemistry and biology, 3rd ed, vol 5. Elsevier, Amsterdam, Netherlands.

12. Huseby DL, Roth JR. 2013. Evidence that a metabolic microcompartment contains and recycles private cofactor pools. J Bacteriol 195:2864–2879. https://doi.org/10.1128/JB.02179-12.

13. Buan NR, Escalante-Semerena JC. 2006. Purification and initial biochemical characterization of ATP:cob(I)alamin adenosyltransferase (EutT) enzyme of *Salmonella enterica*. J Biol Chem 281:16971–16977. https://doi.org/10.1074/jbc.M603069200.

14. Costa FG, Escalante-Semerena JC. 2018. A new class of EutT ATP:co(I)rrinoid adenosyltransferases found in *Listeria monocytogenes* and other *Firmicutes* does not require a metal ion for activity. Biochemistry 57: 5076–5087. https://doi.org/10.1021/acs.biochem.8b00715.

15. Moore TC, Mera PE, Escalante-Semerena JC. 2014. The EutT enzyme of *Salmonella enterica* is a unique ATP:cob(I)alamin adenosyltransferase metalloprotein that requires ferrous ions for maximal activity. J Bacteriol 196: 903–910. https://doi.org/10.1128/JB.01304-13.

16. Buan NR, Suh SJ, Escalante-Semerena JC. 2004. The *eutT* gene of *Salmonella enterica* encodes an oxygen-labile, metal-containing ATP:corrinoid adenosyltransferase enzyme. J Bacteriol 186:5708–5714. https://doi.org/10.1128/JB.186.17.5708-5714.2004.

17. Sheppard DE, Penrod JT, Bobik T, Kofoid E, Roth JR. 2004. Evidence that a B$_{12}$-adenosyl transferase is encoded within the ethanolamine operon of *Salmonella enterica*. J Bacteriol 186:7635–7644. https://doi.org/10.1128/JB.186.22.7635-7644.2004.

18. Schubert HL, Hill CP. 2006. Structure of ATP-bound human ATP:cobalamin adenosyltransferase. Biochemistry 45:15188–15196. https://doi.org/10.1021/bi061396f.

19. Mera PE, Maurice MS, Rayment I, Escalante-Semerena JC. 2007. Structural and functional analyses of the human-type corrinoid adenosyltransferase (PduO) from *Lactobacillus reuteri*. Biochemistry 46:13829–13836. https://doi.org/10.1021/bi701622j.

20. Johnson CL, Pechonick E, Park SD, Havemann GD, Leal NA, Bobik TA. 2001. Functional genomic, biochemical, and genetic characterization of the *Salmonella pduO* gene, an ATP:cob(I)alamin adenosyltransferase gene. J Bacteriol 183:1577–1584. https://doi.org/10.1128/JB.183.5.1577-1584.2001.

21. Escalante-Semerena JC. 2007. Conversion of cobinamide into adenosylcobamide in bacteria and archaea. J Bacteriol 189:4555–4560. https://doi.org/10.1128/JB.00503-07.

22. Heritier C, Poirel L, Nordmann P. 2006. Cephalosporinase over-expression resulting from insertion of IS*Aba1* in *Acinetobacter baumannii*. Clin Microbiol Infect 12:123–130. https://doi.org/10.1111/j.1469-0691.2005.01320.x.

23. Potron A, Vuillemenot J-B, Puja H, Triponney P, Bour M, Valot B, Amara M, Cavalié L, Bernard C, Parmeland L, Reibel F, Larrouy-Maumus G, Dortet L, Bonnin RA, Plésiat P. 2019. IS*Aba1*-dependent overexpression of *eptA* in

clinical strains of *Acinetobacter baumannii* resistant to colistin. J Antimicrob Chemother 74:2544–2550. https://doi.org/10.1093/jac/dkz241.

24. Segal H, Nelson EC, Elisha BG. 2004. Genetic environment and transcription of *ampC* in an *Acinetobacter baumannii* clinical isolate. Antimicrob Agents Chemother 48:612–614. https://doi.org/10.1128/AAC.48.2.612-614.2004.

25. Segal H, Thomas R, Elisha BG. 2003. Characterization of class 1 integron resistance gene cassettes and the identification of a novel IS-like element in *Acinetobacter baumannii*. Plasmid 49:169–178. https://doi.org/10.1016/S0147-619X(03)00011-8.

26. Corvec S, Caroff N, Espaze E, Giraudeau C, Drugeon H, Reynaud A. 2003. AmpC cephalosporinase hyperproduction in *Acinetobacter baumannii* clinical strains. J Antimicrob Chemother 52:629–635. https://doi.org/10.1093/jac/dkg407.

27. Choudhary S, Quin MB, Sanders MA, Johnson ET, Schmidt-Dannert C. 2012. Engineered protein nano-compartments for targeted enzyme localization. PLoS One 7:e33342. https://doi.org/10.1371/journal.pone.0033342.

28. Hull WE, Mauck L, Babior BM. 1975. Mechanism of action of ethanolamine ammonia-lyase, an adenosylcobalamin-dependent enzyme. Proton nuclear magnetic resonance studies of the binding of adenine nucleosides and substrate to ethanolamine ammonia-lyase. J Biol Chem 250:8023–8029. https://doi.org/10.1016/S0021-9258(19)40810-7.

29. Escalante-Semerena JC, Warren MJ. 5 August 2008, posting date. Biosynthesis and use of cobalamin (B$_{12}$). EcoSal Plus 2013 https://doi.org/10.1128/ecosalplus.3.6.3.8.

30. Escalante-Semerena JC, Suh SJ, Roth JR. 1990. *cobA* function is required for both de novo cobalamin biosynthesis and assimilation of exogenous corrinoids in *Salmonella typhimurium*. J Bacteriol 172:273–280. https://doi.org/10.1128/jb.172.1.273-280.1990.

31. O'Toole GA, Escalante-Semerena JC. 1993. *cobU*-dependent assimilation of nonadenosylated cobinamide in *cobA* mutants of *Salmonella typhimurium*. J Bacteriol 175:6328–6336. https://doi.org/10.1128/jb.175.19.6328-6336.1993.

32. Chan CH, Escalante-Semerena JC. 2011. ArsAB, a novel enzyme from *Sporomusa ovata* activates phenolic bases for adenosylcobamide biosynthesis. Mol Microbiol 81:952–967. https://doi.org/10.1111/j.1365-2958.2011.07741.x.

33. Fan C, Cheng S, Liu Y, Escobar CM, Crowley CS, Jefferson RE, Yeates TO, Bobik TA. 2010. Short N-terminal sequences package proteins into bacterial microcompartments. Proc Natl Acad Sci U S A 107:7509–7514. https://doi.org/10.1073/pnas.0913199107.

34. Anderson PJ, Lango J, Carkeet C, Britten A, Kräutler B, Hammock BD, Roth JR. 2008. One pathway can incorporate either adenine or dimethylbenzimidazole as an α-axial ligand of B$_{12}$ cofactors in *Salmonella enterica*. J Bacteriol 190:1160–1171. https://doi.org/10.1128/JB.01386-07.

35. Rowley CA, Anderson CJ, Kendall MM. 2018. Ethanolamine influences human commensal *Escherichia coli* growth, gene expression, and competition with enterohemorrhagic *E. coli* O157:H7. mBio 9:e01429-18. https://doi.org/10.1128/mBio.01429-18.

36. Anderson CJ, Kendall MM. 2016. Location, location, location. *Salmonella* senses ethanolamine to gauge distinct host environments and coordinate gene expression. Microb Cell 3:89–91. https://doi.org/10.15698/mic2016.02.479.

37. Corbella X, Pujol M, Ayats J, Sendra M, Ardanuy C, Dominguez MA, Linares J, Ariza J, Gudiol F. 1996. Relevance of digestive tract colonization in the epidemiology of nosocomial infections due to multiresistant Acinetobacter baumannii. Clin Infect Dis 23:329–334. https://doi.org/10.1093/clinids/23.2.329.

38. Bertani G. 1951. Studies on lysogenesis. I. The mode of phage liberation by lysogenic *Escherichia coli*. J Bacteriol 62:293–300. https://doi.org/10.1128/jb.62.3.293-300.1951.

39. Bertani G. 2004. Lysogeny at mid-twentieth century: P1, P2, and other experimental systems. J Bacteriol 186:595–600. https://doi.org/10.1128/JB.186.3.595-600.2004.

40. Davis RW, Botstein D, Roth JR. 1980. Advanced bacterial genetics: a manual for genetic engineering. Cold Spring Harbor Laboratory Press, Cold Spring Harbor, NY.

41. Berkowitz D, Hushon JM, Whitfield HJ, Jr, Roth J, Ames BN. 1968. Procedure for identifying nonsense mutations. J Bacteriol 96:215–220. https://doi.org/10.1128/jb.96.1.215-220.1968.

42. Tucker AT, Powers MJ, Trent MS, Davies BW. 2019. RecET-mediated recombineering in *Acinetobacter baumannii*. Methods Mol Biol 1946:107–113. https://doi.org/10.1007/978-1-4939-9118-1_11.

43. Datsenko KA, Wanner BL. 2000. One-step inactivation of chromosomal genes in *Escherichia coli* K-12 using PCR products. Proc Natl Acad Sci U S A 97:6640–6645. https://doi.org/10.1073/pnas.120163297.

44. VanDrisse CM, Escalante-Semerena JC. 2016. New high-cloning-efficiency vectors for complementation studies and recombinant protein overproduction in *Escherichia coli* and *Salmonella enterica*. Plasmid 86:1–6. https://doi.org/10.1016/j.plasmid.2016.05.001.

45. Tucker AT, Nowicki EM, Boll JM, Knauf GA, Burdis NC, Trent MS, Davies BW. 2014. Defining gene-phenotype relationships in *Acinetobacter baumannii* through one-step chromosomal gene inactivation. mBio 5:e01313-14. https://doi.org/10.1128/mBio.01313-14.

46. Balch WE, Wolfe RS. 1976. New approach to the cultivation of methanogenic bacteria: 2-mercaptoethanesulfonic acid (HS-CoM)-dependent growth of *Methanobacterium ruminantium* in a pressurized atmosphere. Appl Environ Microbiol 32:781–791. https://doi.org/10.1128/aem.32.6.781-791.1976.

47. Ratzkin P, Roth JR. 1978. Cluster of genes controlling proline degradation in *Salmonella typhimurium*. J Bacteriol 133:744–754. https://doi.org/10.1128/jb.133.2.744-754.1978.

48. Laemmli UK. 1970. Cleavage of structural proteins during the assembly of the head of bacteriophage T4. Nature 227:680–685. https://doi.org/10.1038/227680a0.

49. Stead MB, Agrawal A, Bowden KE, Nasir R, Mohanty BK, Meagher RB, Kushner SR. 2012. RNAsnap: a rapid, quantitative and inexpensive, method for isolating total RNA from bacteria. Nucleic Acids Res 40:e156. https://doi.org/10.1093/nar/gks680.